Vorticity enhancement in thermal counterflow of superfluid helium

P. Hrubcová, P. Švančara, and M. La Mantia*
Faculty of Mathematics and Physics, Charles University, Ke Karlovu 3, 121 16 Prague, Czech Republic

(Received 19 December 2017; published 15 February 2018)

The dynamics of relatively small particles in steady-state thermal counterflow of superfluid ^{4}He (He II) is experimentally investigated by using the particle tracking velocimetry technique. We find that, close to the heat source, the mean distance between quantized vortices, representing the quantum length scale of the flow, is apparently about one order of magnitude smaller than that expected in the bulk, at the same temperature and heat flux. Possible physical mechanisms leading to this significant vorticity enhancement in the heater proximity are discussed and strongly support the view that the geometry of the channel where thermal counterflow occurs has a relevant influence on the observed flow features. Boundary and entrance effects, which have received little attention to date, should therefore be included in a comprehensive description of He II turbulent flows.

DOI: 10.1103/PhysRevB.97.064512

I. INTRODUCTION

Wall-bounded turbulent flows of viscous fluids, such as water or air, have been studied for many years [1–3] mainly because it was recognized early that the influence of solid boundaries on the development of turbulent flows cannot be neglected if one aims at understanding relevant physical mechanisms, e.g., those leading to the generation of vorticity, whose dynamics plays a crucial role in defining the properties of classical turbulence [4].

Similarly, features of turbulent flows of superfluid ^{4}He (He II) can be said to be determined by the corresponding vorticity dynamics, which, above 1 K, as in the present study, results from the interactions between the quantized vortex tangle and the two-component fluid [5–7]. On the phenomenological level, this quantum liquid can be viewed as consisting of two fluids. The gas of thermal excitations—the viscous normal component—carries the entire entropy content of the liquid, while the superfluid component is assumed inviscid and its circulation is quantized in units of the quantum of circulation $\kappa = 9.97 \times 10^{-8}$ m^2/s [8]. Singly quantized vortices may therefore exist in superfluid ^{4}He and their dynamics not only defines the properties of quantum turbulence in He II but also highlights striking similarities as well as distinct differences with turbulent flows of viscous fluids (see, e.g., Švančara and La Mantia [9] and references therein).

However, the effect of solid boundaries on the development of quantum flows has received little attention to date, as pointed out in Ref. [10], and only recently a number of studies have addressed this open problem, see, among others, Stagg *et al.* [11] and La Mantia [12]. In the latter experimental work it has been specifically reported that, in steady-state thermal counterflow of superfluid ^{4}He, quantized vortices are not homogenously distributed in the channel where the quantum flow occurs and that they preferentially concentrate close to its walls, in agreement with previous numerical [13–20] and experimental [21–23] investigations on various types of He II flows. In short, it was found that boundary layers may also exist in quantum flows, although, due to the presence of quantized vortices, some of their features appear to be significantly different from those attributed to wall-bounded flows of viscous fluids, i.e., our understanding of turbulent flows of superfluid ^{4}He is currently being reshaped by this emerging line of scientific enquiry.

The present study addresses the same problem—the boundary influence on the development of He II turbulent flows—from a different perspective. We wanted to clarify if the distance from the flow source has any effect on the observed flow properties because, to the best of our knowledge, this had yet to be thoroughly investigated in the case of quantum flows. Indeed, as pointed out in Ref. [10], results obtained at different distances from the quantum flow source have been often compared assuming implicitly that the latter distances do not play any role in the flow development, although it is well known that channel flows of viscous fluids can be considered to be fully developed solely at a certain distance from the flow source, called entrance length, which depends not only on the fluid velocity but also the channel geometry (e.g., on its cross-section shape) and is of the order of 25 diameters for pipe flows [21].

We choose for these investigations the most common type of He II quantum flow, i.e., thermal counterflow, and we use the same channel, of square cross section, that we employed in previous experiments (see, e.g., La Mantia *et al.* [24] and references therein). On the basis of the large-scale two-fluid model mentioned above, it is possible to say that, once the heater (the flow source) is switched on, the normal component flows away from the heater, while the superfluid component moves in the opposite direction, toward the heat source, in order to conserve the null mass flow rate. Note in passing that, in mechanically driven flows of He II, the fluid components are expected to be locked together, i.e., to flow in the same direction, at large enough length scales, as discussed, e.g., in Ref. [9].

We visualize the motions of relatively small particles suspended in the liquid, by using the particle tracking velocimetry technique [25], in the heater proximity, about 5 times closer to the flow source than in previous studies, and compare the obtained statistical distributions of the particle velocities with

*lamantia@nbox.troja.mff.cuni.cz

those calculated in the bulk, that is, as far away as possible from solid boundaries [12,24]. We take advantage of the fact that the velocity distribution shape depends on the length scale probed by the particles, as clearly shown experimentally by La Mantia and Skrbek [26].

If the probed scale is smaller than the mean distance s_q between quantized vortices, representing the quantum length scale of the flow, the distributions are characterized by power-law tails, which gradually disappear as the length scale is increased, until, at scales of the order of s_q, the distribution form becomes nearly Gaussian and remains approximately unchanged at larger scales, similarly to what is observed in turbulent flow of viscous fluids, in the inertial range, see, e.g., Ref. [27].

It follows therefore that, by looking at the distribution shape (i.e., at its flatness) as a function of the probed scale, it is possible to find the smallest scale corresponding to a classical-like distribution form and, consequently, to say that the latter scale is of the same order of the mean distance s_q between quantized vortices. This approach has been already applied to study thermal counterflow in the wall region [12] and it is here employed to investigate another boundary of the same flow, that is, the heat source.

In summary, from the obtained experimental results, presented below, it can be argued that the quantum length scale in the heater proximity is approximately one order of magnitude smaller than that expected in the bulk, i.e., at about two hydraulic diameters away from the heater, at the same temperature and applied heat flux. Possible physical explanations of this significant vorticity enhancement are then discussed and reinforce the view that the geometry of the channel where quantum flows occur have an appreciable influence on the flow development.

II. METHODS

We employ the Prague low-temperature flow visualization setup, described in detail in our previous publications, see Ref. [9] and references therein. Its main part is a low-loss liquid ^{4}He cryostat and its optical tail constitutes our experimental volume, of square cross section (50 mm sides) and 300 mm high. A 25 mm diameter window is located on the middle of each tail side, 10 cm above the experimental volume bottom.

The particles suspended in the liquid are made of solid deuterium (or hydrogen) and their mean size is of few micrometers, see Refs. [9,26] for typical particle size distributions. They are generated by mixing helium and deuterium (or hydrogen) gasses at room temperature, in a volume ratio of approximately 100 to 1, and by injecting the mixture into the helium bath (gaseous deuterium, or hydrogen, solidifies during the injection). The imposed flow induces the particles to move and we illuminate them by a laser sheet, approximately 1 mm thick and 10 mm high. The particle time-dependent positions are captured by a digital camera, situated perpendicularly to the laser sheet and sharply focused on the illuminated plane (the camera and laser are outside the experimental volume, at room temperature; two optical ports are used for the laser sheet and one for the camera).

Experiments are performed in a vertical glass channel, of square cross section (25 mm sides) and 100 mm high, inserted inside the tail, as far away as possible from the volume vertical walls, i.e., in the tail middle; a flat heater is placed on the channel bottom to generate the flow; see Ref. [10] for a picture of the channel.

The 1 Mpx CMOS camera field of view (13 mm wide and 8 mm high) is situated in the middle of the channel and its vertical sides are about 6 mm away from the channel vertical walls (the laser sheet goes through the tail middle part). For the experiments in the heater proximity, discussed here, the field of view is placed approximately 1 mm above the flow source, while, in the case of the bulk experiments [26,28], employed as a term of comparison, the field of view is located about 5 cm away from the heater, that is, in the channel middle region, two hydraulic diameters above the flow source [10].

Bulk (heater proximity) movies are collected at constant bath temperature, at 400 fps (500 fps), approximately 1 min (few seconds) after the fluid is set into motion, and are subsequently processed. We detect particle positions and link them into trajectories by using an open-source software [29]. We obtain, in each experimental condition, about 10^6 particle positions (which are also linearly smoothed) and keep for further processing solely tracks with at least five points (on each image we find typically 100 particles; trajectories with up to few hundred points are computed). The time-resolved positions are then linearly differentiated to obtain the corresponding velocities, following a procedure similar to that outlined in Ref. [9].

The liquid temperature T and the applied heat flux q, which characterize each experimental run, see Table I, are used to calculate the thermal counterflow velocity

$$v_{ns} = v_n - v_s = \frac{q}{\rho S T}\left(1 + \frac{\rho_n}{\rho_s}\right) = \frac{q}{\rho_s S T}, \qquad (1)$$

where v_n and v_s indicate the normal fluid and superfluid velocities, respectively (we assume here that $v_n > 0$ and $v_s < 0$). The total density ρ of the fluid, defined as the sum of the densities of its normal (ρ_n) and superfluid (ρ_s) components, depends weakly on temperature, while the densities ρ_n and ρ_s display much stronger temperature dependencies (He II can be often considered entirely superfluid at temperatures below 1 K); S denotes the entropy per unit mass, tabulated, together with other fluid properties, in Ref. [8] (note in passing that liquid ^{4}He becomes superfluid below the transition temperature

TABLE I. Experimental conditions. D1 to D4: thermal counterflow in the heater proximity, with deuterium particles; BH: bulk thermal counterflow, with hydrogen particles; BD: bulk thermal counterflow, with deuterium particles. Temperature T (K); applied heat flux q (W/m^2); thermal counterflow velocity v_{ns} (mm/s) [Eq. (1)]; Reynolds number Re [Eq. (2)]; mean particle velocity V (mm/s), at the smallest time t between particle positions; quantum length scale s_q (μm) [Eq. (3)]; quantum time t_q (ms) [Eq. (5)].

Case	T	q	v_{ns}	$Re/10^3$	V	s_q	t_q
D1	1.24	23	2.2	4.0	2.2	674	305
D2	1.40	54	2.2	5.2	2.4	409	168
D3	1.75	235	2.7	7.6	2.3	177	76
D4	1.95	234	1.9	5.1	1.6	183	113
BH	1.77	612	6.8	19.0	2.4	70	29
BD	1.77	608	6.7	18.8	3.9	70	18

$T_\lambda \approx 2.17$ K, at the saturated vapor pressure; above T_λ it is a classical viscous fluid, known as He I).

Additionally, following Refs. [10,21], our measurements can be characterized by the Reynolds number

$$Re = \frac{\rho v_{ns} D}{\mu}, \tag{2}$$

where $D = 25$ mm denotes the channel hydraulic diameter and μ indicates the dynamic viscosity of the He II normal component, also tabulated in Ref. [8], see again Table I.

III. LENGTH AND TIME SCALES

The mean particle size, which, as mentioned above, is of few micrometers, can be considered to be the smallest length scale that we are able to access experimentally. However, a particle may travel a distance larger than its size between two consecutive positions. The length scale s_p probed by the particles can therefore be larger than the mean particle size, and it is estimated here as the mean particle velocity V times the time t between two consecutive positions. Note that the mean particle velocity V has been obtained at the smallest t, which is 2.5 ms (2 ms) for bulk (heater proximity) cases, and that it is possible to increase s_p artificially by removing particle positions from the trajectories obtained at the smallest t, in order to access larger flow scales [26].

The physical scales of the studied flow have then to be compared with the scales probed by the particles. The size of the quantized vortex core, which is of the order of 10^{-10} m, i.e., much smaller than typical particle sizes, cannot currently be resolved by visualization methods. The mean distance s_q between quantized vortices, representing the quantum length scale of the flow, is instead of the order of 100 μm, in the range of investigated parameters, see below. In other words, the used particles can probe scales smaller than s_q, if the movies are taken fast enough.

Following previous studies [12,24,26], we also introduce here the scale ratio $R = s_p/s_q$, between the experimental and quantum scales, and, as detailed below, we obtain values of s_p straddling about two orders of magnitude across s_q.

The quantum length scale s_q is set equal to $1/\sqrt{L}$, where L indicates the vortex line density, which is the total length of quantized vortices per unit volume and is often used to characterize quantum flows. As it is generally assumed that L is proportional to the square of the counterflow velocity v_{ns}, we can write

$$s_q = 1/(\gamma v_{ns}), \tag{3}$$

where the temperature-dependent parameter γ is known from experiments and numerical simulations with an accuracy of about 30%; see, for example, Ref. [30] and references therein. For the sake of consistency with our previous works, the γ values reported in Ref. [31], which were obtained numerically in the bulk, are employed here, following Ref. [24].

As apparent from Table I, the smallest values of s_p (obtained as V times the minimum time between particle positions) range from 3 to 10 μm, i.e., they are appreciably smaller than the estimated values of quantum length scale, which, as mentioned above, are of the order of 100 μm.

R can also be seen as the ratio between two characteristic times of the investigated flow [26]. The time t_q needed to a particle to travel, with a velocity V, a distance equal to s_q can be calculated as s_q/V, and we can then write

$$R = \frac{s_p}{s_q} = \frac{Vt}{s_q} = \frac{t}{t_q} = (\gamma v_{ns} V)t, \tag{4}$$

where t denotes the time between consecutive particle positions and the quantum time

$$t_q = 1/(\gamma v_{ns} V). \tag{5}$$

Corresponding quantum times are listed in Table I and are significantly larger than the smallest time between particle positions, equal to 2.5 ms (2 ms) for bulk (heater proximity) runs. We can therefore say that, in the present case, flow scales smaller than relevant quantum scales can be accessed.

Another relevant scale is the diffusion time t_d, which is a measure of the system thermal relaxation and can be said to be proportional to the time needed to reach the steady state, at a distance H from the heat source [32]. It can be estimated, to a first approximation, following Ref. [32], as H^2/D, where D denotes the fluid thermal diffusivity, equal to $k/(\rho C)$; the corresponding thermal conductivity k, which, in general, is a function of temperature and pressure, can also be said to be inversely proportional to the square of the applied heat flux, while the liquid heat capacity C can be estimated from the temperature dependence of the fluid enthalpy, at the saturated vapor pressure; we have used here relevant values tabulated in Ref. [32]. We find that, for an applied heat flux of 1 kW/m^2 and a diffusion length of 10 cm, the maximum value of t_d is about 3 ms, in the range of investigated temperatures (note that the diffusion time is proportional to the square of the heat flux and that the fluid thermal conductivity has a peak at approximately 1.92 K).

It follows consequently that, as movies were collected at least few seconds after the heater was switched on, the investigated flows can be said to have reached the steady state. Similarly, the diffusion time estimate justifies the use of the tail cross section area for the calculation of q, from the measured dissipated power.

Additionally, it was shown by La Mantia [10] that, in the same channel, the turbulence onset occurs at $v_{ns} \approx 1$ mm, corresponding to $Re \approx 2300$, which is a value consistent with critical Reynolds numbers observed in pipe flows of viscous fluids [2]. As the lowest Re probed in the present experiments is about 4000, see Table I, the studied flows can also be considered turbulent ones.

IV. VELOCITY FLATNESS

In order to access scales larger than the smallest one, corresponding to the minimum time between particle positions, we follow the procedure outlined by La Mantia and Skrbek [26] and employed in subsequent studies, see, e.g., Ref. [12]. We remove particle positions from the trajectories obtained at the smallest time, i.e., we increase t in Eq. (4), and calculate the corresponding particle velocities. We then compute the velocity statistical distributions, at increasing values of R, and observe the gradual disappearance of the distribution power-law tails, which, as discussed, e.g., in Ref. [24], can

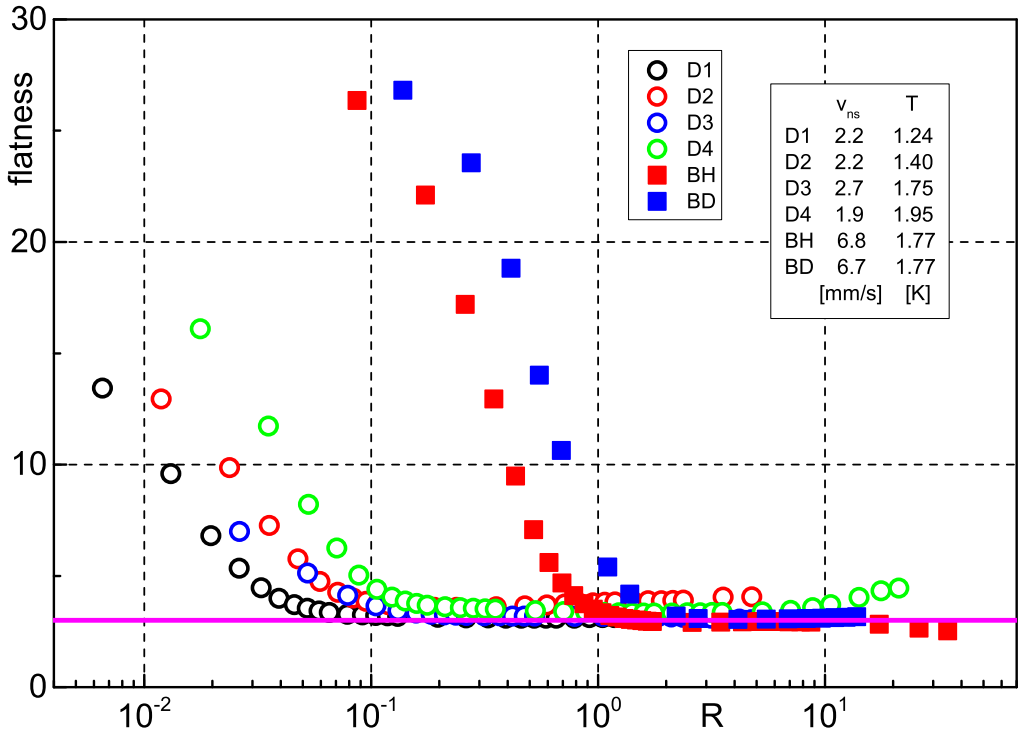

FIG. 1. Flatness of the $(u - u_m)/u_{sd}$ distribution as a function of the scale ratio R, Eq. (4), where u_m and u_{sd} indicate the mean value and the standard deviation of the instantaneous dimensional velocity u in the horizontal direction, respectively (u is positive if directed from the left to the right of the field of view); at least 10^5 velocities. Circles and squares denote counterflow data obtained in the proximity of the heater and in the bulk, respectively, see also Table I. Magenta line: Flatness of the Gaussian distribution.

be explained by taking into account the interactions between particles and quantized vortices.

We already reported [26,28] that, in the case of bulk counterflow, for $R \geqslant 1$, the velocity distributions display nearly Gaussian forms, similarly to what is observed in turbulent flows of viscous fluids, see, e.g., [27], and that the outcome is especially evident if we plot the distribution flatness (i.e., its fourth moment) as a function of the scale ratio R (the flatness of the standard Gaussian distribution is equal to 3). In other words, at scales larger than s_q, the velocity distribution form is classical-like, while, at the smallest scales, it is characterized by power-law tails, which result in significantly larger flatness values, up to 30.

We then apply this approach to the movies obtained in the heater proximity and the rather surprising outcome is displayed in Fig. 1, for the particle velocities in the horizontal direction, perpendicular to the imposed counterflow (note that, as in previous studies, see, e.g., Ref. [12], we focus here on the horizontal velocities mainly because their small-scale statistical distributions display clearer power-law tails, due to the fact that the mean flow is in the vertical direction).

It is apparent that the distribution flatness reaches the Gaussian value at $R \approx 1$ for the bulk case with hydrogen particles (BH). It follows that the corresponding quantum length scale s_q, which we used in our R estimate, is indeed of the same order of the actual one and we therefore employ in the following the bulk hydrogen case as a term of comparison.

The most striking outcome of Fig. 1 is that the flatness values obtained close to the heater reach the Gaussian one at R values about one order of magnitude smaller than that expected. As the length scale probed by the particles does not change appreciably in the present conditions, at constant R, the outcome can solely be explained by saying that the quantum length scale estimated on the basis of bulk numerical simulations [31] is not the correct one in the heater proximity. The result then apparently indicates that, close to the heater, quantized vortices are, on average, approximately 10 times closer to each other than in the bulk, i.e., we argue that, in the heater proximity, the vortex tangle is appreciably denser than in the bulk, at the same temperature and applied heat flux.

In order to appreciate the outcome in a more quantitative way, we introduce the effective scale ratio

$$R_1 = cR = c(\gamma v_{ns} V)t, \tag{6}$$

where the parameter c can be seen as a first-order measure of the observed vorticity enhancement in the heater proximity, and we plot in Fig. 2 the flatness of the velocity distribution as a function of this effective ratio. It is evident that the values of c close to the heater are about one order of magnitude larger than those found in the bulk.

We can also note in Fig. 2 that the c value obtained in the bulk with deuterium particles (BD) is smaller than that of the reference case (BH). As pointed out by La Mantia [12], this can be explained by taking into account the fact that deuterium particles are expected to accelerate about two times less then hydrogen ones, due to inertia and added mass effects [28]. In other words, the steady-state properties of the vortex tangle probed by deuterium and hydrogen particles are the same but deuterium particles effectively experience a less dense tangle.

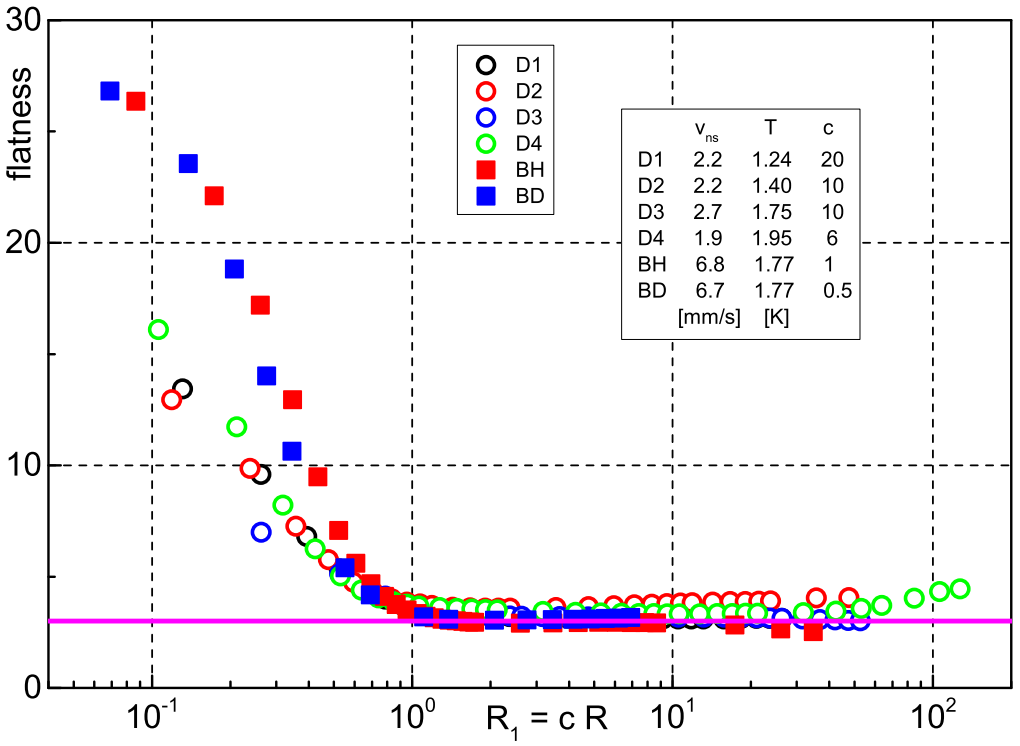

FIG. 2. Flatness of the $(u - u_m)/u_{sd}$ distribution as a function of the effective scale ratio $R_1 = cR$, Eq. (6). The obtained c values are shown in the figure. Symbols as in Fig. 1, see also Table I.

It then follows that the c values shown in Fig. 2 for the heater proximity cases should be regarded as a conservative estimate of the corresponding quantum scale decrease because, close to the heat source, we used only deuterium particles.

The observed decrease of the parameter c as the temperature is increased, at approximately constant counterflow velocity, can be related to the fact that γ increases with T [30,31], that is, at constant R_1, the increase of γ could be compensated by the corresponding decrease of c, see Eq. 6.

Additionally, it is shown in Table I that, for the heater proximity cases, $v_{ns} \approx V$, while, in the bulk, i.e., at two hydraulic diameters away from the flow source, the mean particle velocity is appreciably smaller than the counterflow velocity. The outcome can be explained after noting that, as reported by La Mantia [10], also in the bulk, $v_{ns} \approx V$ for counterflow velocities up to about 2 mm/s. It is indeed known that particles are less likely to be trapped onto quantized vortices, i.e., to move at a relatively constant velocity, at large enough v_{ns} [10,33].

This also means that, at constant temperature, the parameter c should decrease as the counterflow velocity is increased, because, at constant R_1, the increase of $v_{ns}V$ could be balanced by the corresponding decrease of c, see Eq. (6). As apparent from Table I, the present data sets do not allow us to verify this argument, that is, movies at counterflow velocities larger than those reported here should be collected. However, it should be kept in mind that, if v_{ns} is increased, the corresponding quantum scale decreases, see Eq. (3), i.e., it could not be possible to access scales smaller than s_q—and to estimate c—by employing the same particles of micrometer size.

Additionally, we can notice in Fig. 2 that, for $R_1 < 1$, the flatness slope in the bulk is steeper than that close to the heater. As already suggested in Ref. [12], this could be due to the occurrence of wall-bounded vortical flows, that is, the outcome might indicate a more pronounced classical-like behavior of the quantum flow in boundary regions, resulting from the finite size of the particles and the denser vortex tangle. As in the case of the temperature and heat flux dependence of the parameter c, further experiments are required to clarify the issue, which, however, is not the focus of the present work.

Indeed, our aim here is to report on the apparent decrease of the quantum length scale in the heater proximity and in the following we speculate on the possible physical origins of the observed vorticity enhancement and on their implications.

V. DISCUSSION

We start from Eq. (3), which relates the vortex line density L to the counterflow velocity. The latter is calculated from Eq. (1), that is, it solely depends on the bath temperature and on the applied heat flux. The counterflow velocity v_{ns} is therefore a global quantity, used to characterize the studied flow, and Eq. (3) is, in general, not expected to hold locally. In other words, if we take a region of the (steady-state) flow field and measure in that volume the total length of vortex lines, we will find that, by using the γ values reported in the literature, Eq. (3) is strictly satisfied only if we are far enough from the flow boundaries.

Indeed, our experimental results demonstrate the previous statement on the global validity of Eq. (3) and support its inapplicability in boundary regions. It also follows that the reason why γ values are known with an accuracy of about 30% [30] could be related to the fact that they were obtained at different distances from the channel walls and the flow source,

that is, the values of the temperature-dependent parameter γ reported in the literature might be affected by the position within the channel where γ was actually measured.

Note in passing that $\sqrt{L}$ is usually set equal to $\gamma(v_{ns} - v_c)$, where the velocity v_c, indicating the onset of the turbulent state, is, as mentioned above, about 1 mm/s for the present channel. We, nevertheless, decided not to account for the effect here because this would have resulted in even larger values of c, see Eq. (6), i.e., the observed decrease of the quantum scale in the heater proximity can definitely be regarded as a conservative estimate.

It is now time to propose a physical explanation of our experimental findings, strongly suggesting that in the heater proximity the quantized vortex tangle is appreciably denser than in the bulk. The outcome could be partly justified by taking into account the roughness of our flat heater surface, following, for example, the numerical work by Stagg *et al.* [11]. Due to the atomic size of the quantized vortex core, any surface can indeed be regarded as full of pinning/nucleation sites for the vortices. Additionally, in the case of steady-state thermal counterflow, quantized vortices tend to concentrate close to the channel boundaries, due to the classical behavior of the He II normal component, as discussed, e.g., in Ref. [12].

In the latter experimental study it was found that close to the channel glass wall, at two hydraulic diameters away from the heat source, the vortex tangle appears to be about 1.5 times denser than in the bulk (at the same distance from the heater but further away from the wall, in the middle of the channel). The larger quantum scale decrease we report here could then be partly due to the larger roughness of the heater surface compared to that of the channel vertical wall.

On the other hand, we can say that, far enough from the heat source, the flow of the inviscid superfluid component does not depend on its distance from the wall, while the viscous normal component flows faster in the bulk than in the boundary proximity, due to the influence of the channel walls, as in turbulent flows of viscous fluids, see, for example, Ref. [34]. In other words, we assume here that the normal fluid velocity can vary locally, across the channel width, in regions larger than the mean distance between quantized vortices, while the counterflow velocity v_{ns} remains unchanged. It then follows that quantized vortices tend to concentrate in flow regions characterized by smaller values of local fluid velocity, that is, in the wall proximity.

This argument could also be applied to the steady-state flow occurring in the proximity of the heater, which is a boundary perpendicular to the mean flow direction and not parallel to it, as the vertical glass wall. Note in passing that here we consider the particle horizontal velocities which, in general, are not null, as testified by the corresponding statistical distributions, that is, the flow-induced particle motions suggest that the studied flows of He II might locally be also parallel to the heater and, consequently, promote vortex nucleation [11,35].

We can now assume that, close to the flow source, the boundary layer on the vertical channels walls is less thick than in the bulk region, similarly as in classical flows, where the boundary layer thickness increases with the distance from the channel entrance; see, e.g., Ref. [12] for a simple estimate of the boundary layer thickness based on the Blasius formula. It then follows that, in the heater proximity, the local value of fluid velocity should also be smaller than in the bulk. We could therefore say that quantized vortices would accumulate not only in wall regions but also in the vicinity of the closed end of the channel, where the heater is placed, considering especially that these vortices are carried by the superfluid component, which moves toward the heater.

The temperature difference between the bulk and the heater proximity could also contribute to explain the experimental findings because, if the counterflow velocity is set, the vortex line density should increase with temperature, see again Eq. (3). However, on the basis of the extremely small diffusion times estimated above, we believe that this effect should not play a significant role in the range of investigated parameters, that is, we have assumed here that the fluid temperature does not vary appreciably in the bath. Future experiments should then be devoted to measure the temperature gradient along the channel, as a function of bath temperature and applied heat flux.

We can now conclude our discussion by saying that further studies are needed to verify the proposed physical arguments, for example, to estimate the boundary layer thickness as a function of the distance from the flow source. Additionally, the present experimental findings demonstrate the significant role played by the channel geometry in the development of quantum flows, that is, comparisons between results obtained in different channels, at different distances from the walls and the flow source, should be performed after having assessed quantitatively how the channel geometry influences the investigated flows.

VI. CONCLUSIONS

We have visualized the flow-induced dynamics of relatively small particles suspended in superfluid ^{4}He. We have specifically probed the most common type of He II flow—thermal counterflow—in the heat source proximity, about 5 times closer than in previous studies [10,12,26,28], our aim being to assess the relevance of the distance from the heater in the development of this quantum flow.

We have found that the quantum length scale of the flow—the mean distance between quantized vortices—is apparently one order of magnitude smaller than that expected in the bulk, at the same temperature and applied heat flux, in the range of investigated parameters, i.e., at counterflow velocities of about 2 mm/s—two times larger than the channel turbulence onset velocity [10]—and at temperatures ranging between 1.24 and 1.95 K.

Following Refs. [11,12], we have argued that the observed vorticity enhancement could be due to the heater surface roughness (providing pinning/nucleation sites for the vortices) and to the classical behavior of the He II normal component (which can account for the tendency of quantized vortices to preferentially concentrate away from the flow bulk).

Comparisons with data obtained in the bulk [26,28] have shown that, for the used channel, of square cross section (25 mm sides) and 100 mm high, the entrance length, indicating the distance from the flow source at which the flow can be considered to be fully developed, is smaller than 50 mm, corresponding to two hydraulic diameters, which is a value appreciably smaller than that obtained for pipe flows of viscous fluids [21].

Future studies should then be devoted to address in more detail the specific features of He II wall-bounded flows, in order to clarify possible similarities and differences with turbulent flows of viscous fluids [1–3]. On the one hand, we can indeed say that boundary layers also exist in quantum flows but, on the other hand, we can claim that their origin is more related to the quantized vortex dynamics than to the fluid viscosity.

An associated research route could be to compare thermal counterflow with heat transport mechanisms in classical flows, such as in turbulent Rayleigh-Bénard convection (RBC), see, e.g., the review by Chillà and Schumacher [36]. It is, for example, well known how to estimate the thickness δ of the thermal boundary layer in RBC and, following Ref. [37], we can write

$$\delta = \frac{k\Delta T}{2Q}, \tag{7}$$

where k is the fluid thermal conductivity, ΔT indicates the temperature difference between the parallel bottom and top plates of the convection cell (the fluid is heated from below), and Q denotes the convective heat flux.

For the sake of argument, we can now use Eq. (7) for the present counterflow experiments. If we set $k = 10^6$ W/(m K) and $Q = q = 1$ kW/m^2, following our above estimate of the diffusion time [32], we find that, in order to get $\delta = 10$ mm, comparable to our field of view height, ΔT should be equal to 20 μK. It is then possible to say that, due to the extremely small temperature difference, we should appreciably increase the heat flux in order to access experimentally the thermal boundary layer, if the latter actually exists.

The proposed line of scientific enquiry can then be seen an as additional proof that the investigation of quantum flows is not only interesting in its own right but may also contribute to our general understating of turbulent flows. In other words, as testified by the present work on boundary effects in thermal counterflow, classical fluid mechanics tools may also be useful for the analysis of quantum flows.

ACKNOWLEDGMENTS

We thank D. Duda, P.-E. Roche, M. Rotter, L. Skrbek, and E. Varga for fruitful discussions and valuable help. We acknowledge the support of the Czech Science Foundation under GAČR Grant No. 16-00580S.

[1] I. Marusic, B. J. McKeon, P. A. Monkewitz, H. M. Nagib, A. J. Smits, and K. R. Sreenivasan, Wall-bounded turbulent flows at high Reynolds numbers: Recent advances and key issues, Phys. Fluids **22**, 065103 (2010).

[2] K. Avila, D. Moxey, A. de Lozar, M. Avila, D. Barkley, and B. Hof, The onset of turbulence in pipe flow, Science **333**, 192 (2011).

[3] M. Stanislas, Near wall turbulence: An experimental view, Phys. Rev. Fluids **2**, 100506 (2017).

[4] A. Tsinober, *An Informal Conceptual Introduction to Turbulence* (Springer, Dordrecht, 2009).

[5] W. F. Vinen and J. J. Niemela, Quantum turbulence, J. Low Temp. Phys. **128**, 167 (2002).

[6] L. Skrbek and K. R. Sreenivasan, Developed quantum turbulence and its decay, Phys. Fluids **24**, 011301 (2012).

[7] C. F. Barenghi, L. Skrbek, and K. R. Sreenivasan, Introduction to quantum turbulence, Proc. Natl. Acad. Sci. U.S.A. **111**, 4647 (2014).

[8] R. J. Donnelly and C. F. Barenghi, The observed properties of liquid helium at the saturated vapor pressure, J. Phys. Chem. Ref. Data **27**, 1217 (1998).

[9] P. Švančara and M. La Mantia, Flows of liquid ^{4}He due to oscillating grids, J. Fluid Mech. **832**, 578 (2017).

[10] M. La Mantia, Particle trajectories in thermal counterflow of superfluid helium in a wide channel of square cross section, Phys. Fluids **28**, 024102 (2016).

[11] G. W. Stagg, N. G. Parker, and C. F. Barenghi, Superfluid Boundary Layer, Phys. Rev. Lett. **118**, 135301 (2017).

[12] M. La Mantia, Particle dynamics in wall-bounded thermal counterflow of superfluid helium, Phys. Fluids **29**, 065102 (2017).

[13] A. W. Baggaley and S. Laizet, Vortex line density in counter-flowing He II with laminar and turbulent normal fluid velocity profiles, Phys. Fluids **25**, 115101 (2013).

[14] L. Galantucci and M. Sciacca, Non-classical velocity statistics in counterflow quantum turbulence, Acta Appl. Math. **132**, 273 (2014).

[15] A. W. Baggaley and J. Laurie, Thermal counterflow in a periodic channel with solid boundaries, J. Low Temp. Phys. **178**, 35 (2015).

[16] S. Yui and M. Tsubota, Counterflow quantum turbulence of He-II in a square channel: Numerical analysis with nonuniform flows of the normal fluid, Phys. Rev. B **91**, 184504 (2015).

[17] L. Galantucci, M. Sciacca, and C. F. Barenghi, Coupled normal fluid and superfluid profiles of turbulent helium II in channels, Phys. Rev. B **92**, 174530 (2015).

[18] D. Khomenko, V. S. L'vov, A. Pomyalov, and I. Procaccia, Mechanical momentum transfer in wall-bounded superfluid turbulence, Phys. Rev. B **93**, 134504 (2016).

[19] S. Ikawa and M. Tsubota, Coflow turbulence of superfluid ^{4}He in a square channel: Vortices trapped on a cylindrical attractor, Phys. Rev. B **93**, 184508 (2016).

[20] D. Khomenko, P. Mishra, and A. Pomyalov Coupled dynamics for superfluid ^{4}He in a channel, J. Low Temp. Phys. **187**, 405 (2017).

[21] T. Xu and S. W. Van Sciver, Particle image velocimetry measurement of the velocity profile in He II forced flow, Phys. Fluids **19**, 071703 (2007).

[22] E. Varga, S. Babuin, and L. Skrbek, Second-sound studies of coflow and counterflow of superfluid ^{4}He in channels, Phys. Fluids **27**, 065101 (2015).

[23] A. Marakov, J. Gao, W. Guo, S. W. Van Sciver, G. G. Ihas, D. N. McKinsey, and W. F. Vinen, Visualization of the normal-fluid turbulence in counterflowing superfluid ^{4}He, Phys. Rev. B **91**, 094503 (2015).

[24] M. La Mantia, P. Švančara, D. Duda, and L. Skrbek, Small-scale universality of particle dynamics in quantum turbulence, Phys. Rev. B **94**, 184512 (2016).

[25] W. Guo, M. La Mantia, D. P. Lathrop, and S. W. Van Sciver, Visualization of two-fluid flows of superfluid helium-4, Proc. Natl. Acad. Sci. U.S.A. **111**, 4653 (2014).
[26] M. La Mantia and L. Skrbek, Quantum, or classical turbulence? Europhys. Lett. **105**, 46002 (2014).
[27] M. Mordant, E. Lévêque, and J.-F. Pinton, Experimental and numerical study of the Lagrangian dynamics of high Reynolds turbulence, New J. Phys. **6**, 116 (2004).
[28] M. La Mantia and L. Skrbek, Quantum turbulence visualized by particle dynamics, Phys. Rev. B **90**, 014519 (2014).
[29] I. F. Sbalzarini and P. Koumoutsakos, Feature point tracking and trajectory analysis for video imaging in cell biology, J. Struct. Biol. **151**, 182 (2005).
[30] S. Babuin, M. Stammeier, E. Varga, M. Rotter, and L. Skrbek, Quantum turbulence of bellows-driven ^{4}He superflow: Steady state, Phys. Rev. B **86**, 134515 (2012).
[31] Y. A. Sergeev, C. F. Barenghi, and D. Kivotides, Motion of micron-size particles in turbulent helium II, Phys. Rev. B **74**, 184506 (2006).
[32] S. W. Van Sciver, *Helium Cryogenics* (Springer, New York, 2012).
[33] M. La Mantia, D. Duda, M. Rotter, and L. Skrbek, Lagrangian accelerations of particles in superfluid turbulence, J. Fluid Mech. **717**, R9 (2013).
[34] H. Schlichting and K. Gersten, *Boundary-Layer Theory* (Springer, Berlin, 2017).
[35] K. W. Schwarz, Phase Slip and Turbulence in Superfluid ^{4}He: A Vortex Mill that Works, Phys. Rev. Lett. **64**, 1130 (1990).
[36] F. Chillà and J. Schumacher, New perspectives in turbulent Rayleigh–Bénard convection, Eur. Phys. J. E **35**, 58 (2012).
[37] N. Shi, M. S. Emran, and J. Schumacher, Boundary layer structure in turbulent Rayleigh–Bénard convection, J. Fluid Mech. **706**, 5 (2012).